

# HDAC2 mediates therapeutic resistance of pancreatic cancer cells via the BH3-only protein NOXA

P Fritsche,<sup>1</sup> B Seidler,<sup>1</sup> S Schüler,<sup>1</sup> A Schnieke,<sup>2</sup> M Göttlicher,<sup>3</sup> R M Schmid,<sup>1</sup> D Saur,<sup>1</sup> G Schneider<sup>1</sup>

► Four supplementary figures are published online only at <http://gut.bmj.com/content/vol58/issue10>

<sup>1</sup> Technische Universität München, Klinikum rechts der Isar, II Medizinische Klinik, Munich, Germany; <sup>2</sup> Technische Universität München, Lehrstuhl für Biotechnologie der Nutztiere, Freising, Germany; <sup>3</sup> Helmholtz Zentrum München, Institut für Toxikologie, Neuherberg, Germany

Correspondence to: Dr G Schneider, Technische Universität München, Klinikum rechts der Isar, II Medizinische Klinik, Ismaninger Str 22, 81675 Munich, Germany; [guenter.schneider@lrz.tum.de](mailto:guenter.schneider@lrz.tum.de)

Revised 19 May 2009  
Accepted 1 June 2009  
Published Online First  
14 June 2009

## ABSTRACT

**Background:** Although histone deacetylase inhibitors (HDACi) are promising cancer therapeutics regulating proliferation, differentiation and apoptosis, molecular pathways engaged by specific HDAC isoenzymes in cancer are ill defined.

**Results:** In this study we demonstrate that HDAC2 is highly expressed in pancreatic ductal adenocarcinoma (PDAC), especially in undifferentiated tumours. We show that HDAC2, but not HDAC1, confers resistance towards the topoisomerase II inhibitor etoposide in PDAC cells. Correspondingly, the class I selective HDACi valproic acid (VPA) synergises with etoposide to induce apoptosis of PDAC cells. Transcriptome profiling of HDAC2-depleted PDAC cells revealed upregulation of the BH3-only protein NOXA. We show that the epigenetically silenced NOXA gene locus is opened after HDAC2 depletion and that NOXA upregulation is sufficient to sensitise PDAC cells towards etoposide-induced apoptosis.

**Conclusions:** In summary, our data characterise a novel molecular mechanism that links the epigenetic regulator HDAC2 to the regulation of the pro-apoptotic BH3-only protein NOXA in PDAC. Targeting HDAC2 will therefore be a promising strategy to overcome therapeutic resistance of PDAC against chemotherapeutics that induce DNA damage.

Although the incidence of pancreatic ductal adenocarcinoma (PDAC) is only 10 in 10<sup>5</sup>, it is the fourth leading cause of cancer-related death. One reason for the poor prognosis of PDAC is the failure of most conventional treatments.<sup>1</sup> Nearly all neoplastic changes during the development of a normal cell to a cancer cell, such as DNA damage, oncogene activation or cell cycle deregulation, are potent inducers of the programmed cell death pathway. Therefore, overcoming the apoptotic failsafe is observed in many cancers and results in cell-intrinsic apoptotic and therapeutic resistance.<sup>1,2</sup> Resistance towards apoptosis is also a hallmark of PDAC and therefore lowering the apoptotic threshold is a therapeutic goal.<sup>3</sup> Several recent studies demonstrated that a sensitiser (lowering the apoptotic threshold)/inducer (activation of the apoptotic machinery) strategy is a potential approach for a rational molecular-based tumour therapy in PDAC (summarised by Hamacher *et al*).<sup>4</sup>

According to phylogenetic analyses and sequence homology, histone deacetylases (HDACs) can be grouped in class I to IV enzymes.<sup>4</sup> The yeast Rpd3 homologous enzymes HDAC 1, 2, 3 and 8 represent class I, and the Hda1 homologous

enzymes HDAC 4, 5, 6, 7, 9 and 10 represent class II HDACs. HDAC11 reveals homology to class I as well as to class II and is therefore grouped in class IV. In contrast to the zinc-dependent catalysis, class III deacetylases (SIRT1-7) use NAD<sup>+</sup> as co-factor and are not inhibited by HDAC inhibitors (HDACi). HDACs contribute to cancer initiation and progression by the regulation of cell cycle progression, epithelial differentiation, angiogenesis, metastasis and apoptosis.<sup>5,6</sup> Therefore, HDACi are promising anti-cancer agents and are now being investigated in clinical studies or are already approved by the US Food and Drug Administration for the treatment of cutaneous T cell lymphoma (SAHA).<sup>7</sup>

In PDAC cells several HDACi were investigated in vitro and found to inhibit proliferation and to induce apoptosis.<sup>8-14</sup> At the molecular level, upregulation of the cell cycle inhibitors p21<sup>Cip1</sup> and p27<sup>Kip1</sup> and downregulation of the cell cycle promoters cyclin D1, cyclin B, c-myc and the S-phase kinase-associated protein 2 (SKP2) were observed in PDAC cells upon treatment with HDACi, explaining the HDACi-induced inhibition of proliferation.<sup>8,9,12,15</sup> With respect to apoptosis, the anti-apoptotic BCL2 family members MCL1 and BCL-X<sub>L</sub> were downregulated and the pro-apoptotic BH3-only proteins BIM, BID and the multi-domain pro-apoptotic BCL2 family member BAX as well as caspase 8 were upregulated upon treatment of PDAC cells with HDACi, contributing to HDACi-induced apoptosis and HDACi-mediated sensitisation towards chemotherapeutics in PDAC cells.<sup>10,11,13,16,17</sup>

Although these diverse molecular changes were described in PDAC cells with the use of various HDACi, which target multiple HDACs, less is known about the non-redundant isoenzyme-specific function of the different HDACs and the pathways engaged in PDAC. In this study we demonstrate that HDAC2 is highly expressed in PDAC and mediates therapeutic resistance by contributing to the epigenetic silencing of the pro-apoptotic NOXA gene.

## MATERIALS AND METHODS

### Cell culture, luciferase assays, plasmids and reagents

MiaPaCa2, Panc1, BxPc3 and DanG cells were cultivated as described.<sup>15,18</sup> Valproic acid (VPA), etoposide and 5-fluorouracil (5-FU) were from EMD Biosciences (San Diego, California, USA), oxaliplatin was from LC Laboratories (Woburn, Massachusetts, USA) and gemcitabine from Lilly

(Indianapolis, Indiana, USA). siRNAs were transfected at a concentration of 50 nmol/l using oligofectamine (Invitrogen, Karlsruhe, Germany). siRNAs were purchased from Eurofins (Ebersberg, Germany). Sequences are available on request. The human NOXA luciferase reporter gene construct was a gift from Dr C Lallemand.<sup>19</sup> Transfections of the NOXA luciferase reporter and luciferase assays were performed as described.<sup>15</sup>

### Statistical methods

All data were obtained from at least three independent experiments performed in triplicate and results are presented as the mean and standard error of the mean. To demonstrate statistical significance a two-tailed Student t test was used. p Values are indicated and \* denotes a p value of at least <0.05. IC<sub>50</sub> values were calculated with GraphPad Prism4 using a non-linear regression model.

### Quantitative reverse-transcriptase polymerase chain reaction

Total RNA was isolated from pancreatic carcinoma cell lines using the RNeasy kit (Qiagen, Hilden, Germany). Quantitative mRNA analyses were performed as previously described using real-time polymerase chain reaction (PCR) analysis.<sup>18</sup> Primer sequences are available on request.

### Cell lysates and western blot

Whole cell lysates were prepared and western blots were done as recently described.<sup>18</sup> The following antibodies were used: HDAC2 (Santa Cruz, Santa Cruz, California, USA), NOXA and MCL1 (Alexis Biochemicals, San Diego, California, USA), cleaved poly (ADP-ribose) polymerase family, member 1 (PARP; BD Biosciences, Heidelberg, Germany), HDAC1 (Upstate, Billerica, Massachusetts, USA) and  $\beta$ -actin (Sigma-Aldrich, Munich, Germany).

### BrdU incorporation, MTT and caspase 3/7 assays

Bromodeoxyuridine (BrdU) incorporation and MTT (3-(4,5-dimethylthiazol-2-yl)-2,5-diphenyltetrazolium bromide) assays were performed using a colorimetric BrdU and MTT assay (Roche Applied Science, Mannheim, Germany). Caspase 3/7 activity was determined using Promega's Caspase Glo 3/7 assay (Promega, Madison, Wisconsin, USA) according to the manufacturer's instructions.

### Gene expression profiling

Gene expression profiling was performed as described.<sup>18</sup> Forty-eight hours after the transfection of a control and a HDAC2-specific siRNA, duplicates of total RNA were prepared using an RNeasy Kit (Qiagen). Labelled cRNA was produced and hybridised onto the Affymetrix GeneChip Human Genome U133 Plus 2.0 set according to Affymetrix standard protocols (Affymetrix, Santa Clara, California, USA). Expression data were analysed using Microarray Suite 5.0. Genes known to contribute to the regulation of apoptosis are presented in table 1.

### Chromatin immunoprecipitation assay

Chromatin immunoprecipitation (ChIP) assays were performed as described.<sup>18</sup> The antibodies used were: rabbit polyclonal IgG as negative control, anti-HDAC2 and anti-RNA polymerase II (Santa Cruz Biotechnology, Santa Cruz, California, USA) and anti-acetyl-histone H3 (Upstate). To ensure linearity, 28–38 cycles were performed, and one representative result out of at least three independent experiments is shown. Primer sequences are available on request.

### Immunohistochemistry

The tissue microarray containing normal and PDAC tissue specimens was purchased from BioCat (Heidelberg, Germany). Immunohistochemistry was performed as described.<sup>20</sup> For HDAC2 immunodetection, formalin-fixed paraffin-embedded tissue sections were dewaxed and placed in a microwave (10 min, 600 W) to recover antigens before incubation with the primary HDAC2 antibody (1:100; Santa Cruz). Primary antibody was followed by a secondary antibody conjugated to biotin (Vector Laboratories, Burlingame, California, USA). Peroxidase conjugated streptavidin was used with 3,3'-diaminobenzidine tetrahydrochloride (Sigma) as chromogen. HDAC2 expression was scored in normal pancreatic tissue and PDAC by two independent observers (DS and GS). A final score (0–300) was established by multiplying the percentage of nuclear HDAC2 labelled cells (0–100%) (five high-power fields; magnification,  $\times 400$ ) with the staining intensity (1, low; 2, moderate; 3, strong staining).

### HDAC2 gene expression: microarray dataset

The Ishikawa microarray data set (GEO accession number: GSE1542) was accessed using the OncoPrint™ Database. The dataset was prepared from pancreatic ductal cell samples, cytologically diagnosed as grade I or II (three samples), grade III (10 samples), grade IV (five samples) or grade V (six samples).<sup>21</sup>

## RESULTS

### HDAC2 is over-expressed in PDAC

To investigate HDAC2 expression in PDAC we performed HDAC2 immunohistochemistry using human tissue microarrays. In normal pancreas, the acinar compartment and islets of Langerhans stain positive for nuclear HDAC2 (fig 1A). The epithelium of small ducts stains negative (fig 1A, upper row, left picture), whereas middle (fig 1A, upper row, right picture) and large ducts (fig 1A, lower row) show low intensive nuclear staining of some cells. In PDAC an intense nuclear staining was observed, especially in moderately differentiated and undifferentiated tumours (fig 1B). Scoring of nuclear HDAC2 expression revealed a significant 2.2-fold upregulation of HDAC2 in PDAC compared to normal duct epithelium ( $p=0.006$ ) (fig 1C). Upregulation of HDAC2 was notably observed in G3 tumours (3.1-fold) ( $p=0.038$ ) (fig 1D). To further validate these expression data, we analysed microarray data published by Ishikawa *et al.*<sup>21</sup> As shown in fig 1E, HDAC2 mRNA expression gradually increases according to the cytological grade, being highest in PDAC (cytological grade V).

### HDAC2 is dispensable for viability and proliferation

To investigate HDAC2 function in PDAC cells, we used RNAi. Figure 2A demonstrates the knockdown of HDAC2 48 and 72 h after transfection of MiaPaCa2 and Panc1 cells with a HDAC2 siRNA. HDAC1 protein expression was not downregulated in HDAC2 siRNA-transfected cells, demonstrating specificity (fig 2A). In viability assays over a time course of 72 h, no significant reduction of viability in HDAC2-depleted MiaPaCa2 and Panc1 cells compared to control cells was observed (fig 2B). Furthermore, BrdU incorporation was not significantly altered up to 72 h after transfection of the HDAC2 siRNA into MiaPaCa2 and Panc1 cells, suggesting that loss of HDAC2 in PDAC cells can be compensated with respect to survival and proliferation (fig 2C).

**Table 1** Regulation of genes of the apoptotic machinery by the histone deacetylase (HDAC)2 knockdown

	Gene ID	Official symbol	Alias	Fold regulation (by HDAC2 knockdown)	
				MiaPaCa2	Panc1
	3066	HDAC2	RPD3	-10.5	-7.9
<b>BCL2 family</b>	4170	MCL1		2	1.3
	598	BCL2L1	BCL-X <sub>L</sub>	1.4	1.1
	596	BCL2		-1.3	1
	597	BCL2A1	A1	1	-1.5
	581	BAX		1.1	1.3
	578	BAK1	BAK	1.2	1.2
	666	BOK		1.1	-2.1
	572	BAD		1.9	1.3
	638	BIK		1.3	-1.1
	637	BID		-1.3	-1.3
	10018	BCL2L11	BIM	1.2	1.5
	90427	BMF		1	1.2
	8739	HRK	DP5, HARAKIRI	1	1.2
	27113	BBC3	PUMA, JFY1	1.1	1
	5366	PMAIP1	NOXA, APR	4.7	4
<b>IAP family</b>	467 1	NAIP	BIRC1	-1.2	-1.1
	330	BIRC3	cIAP2	1.1	-1.1
	329	BIRC2	cIAP1	-1.9	1.6
	331	XIAP	BIRC4	1.8	1.2
	79444	BIRC7	LIVIN	1	1
	57448	BIRC6	APOLLON, BRUCE	1.4	1.4
	332	BIRC5	SURVIVIN	1.2	1.5
<b>Death receptors and adaptors</b>	7132	TNFRSF1A	TNFR1	-1.2	1.1
	7133	TNFRSF1B	TNFR2	-1.1	-1.6
	8797	TNFRSF10A	TRAILR1, DR4	1.4	1.5
	8795	TNFRSF10B	TRAILR2, DR5	2.2	1.5
	8717	TRADD		1.2	-1.7
	8772	FADD	MORT1	1	1
	8837	CFLAR	FLIP	1.2	1.7
<b>Mitochondrial proteins</b>	317	APAF1	CED4	-1.1	1.4
	9131	AIFM1	AIF	1.2	1.5
	56616	DIABOLO	SMAC	-1.1	-1.2
	27429	HTRA2	OMI	-1.1	-1.3

### Loss of HDAC2 sensitises towards etoposide

Since HDACs contribute to therapeutic resistance of cancer cells, we tested the sensitivity of HDAC2-depleted MiaPaCa2 and Panc1 cells towards intrinsic inducers of apoptosis.<sup>6</sup> As shown via Hoechst stains in fig 3A, a significantly increased apoptotic fraction in HDAC2-depleted MiaPaCa2 and Panc1 cells was observed 24 h after treatment with the topoisomerase II inhibitor etoposide in a dose-dependent manner. Consistently, 48 h after etoposide treatment of HDAC2 siRNA-transfected MiaPaCa2 and Panc1 cell viability was significantly reduced (fig 3B). Increased sensitivity of MiaPaCa2 and Panc1 cells towards etoposide was further verified using caspase 3/7 assays. As shown in fig 3C, distinctly increased caspase activation was observed in HDAC2 siRNA-transfected MiaPaCa2 and Panc1 cells after treatment with etoposide in a dose-dependent manner. Accordingly, increased caspase activity led to a pronounced cleavage of the caspase substrate PARP in HDAC2-depleted MiaPaCa2 and Panc1 cells (fig 3D). Furthermore, the inhibitory concentration 50% (IC<sub>50</sub>) for etoposide in HDAC2-depleted MiaPaCa2 and Panc1 cells

was significantly reduced (fig 3E). A similar sensitisation towards etoposide was observed in HDAC2-depleted DanG and BxPc3 cells, arguing for a general mechanism in PDAC cells (supplementary fig 1). Sensitisation towards etoposide was specific for HDAC2, since knockdown of HDAC1 (fig 3F) did not result in increased sensitivity of MiaPaCa2 and Panc1 cells towards etoposide (fig 3G).

### Valproic acid sensitises towards etoposide

To validate the RNAi results, we used the HDACi valproic acid (VPA), since VPA is a class I-specific HDACi and known to deplete HDAC2 via the proteasome.<sup>22 23</sup> VPA-mediated depletion of HDAC2 was also observed in MiaPaCa2 and Panc1 cells (fig 4A). Using up to 1.5 mmol/l VPA, a concentration achievable in therapeutic settings in humans, no reduction of PDAC cell proliferation (fig 4B) or viability (fig 4C) was observed over a time course of 72 h. As in HDAC2-depleted cells, the apoptotic fraction of VPA/etoposide co-treated MiaPaCa2 and Panc1 cells significantly increased compared to etoposide-treated PDAC cells (fig 5A). The sensitising effect of

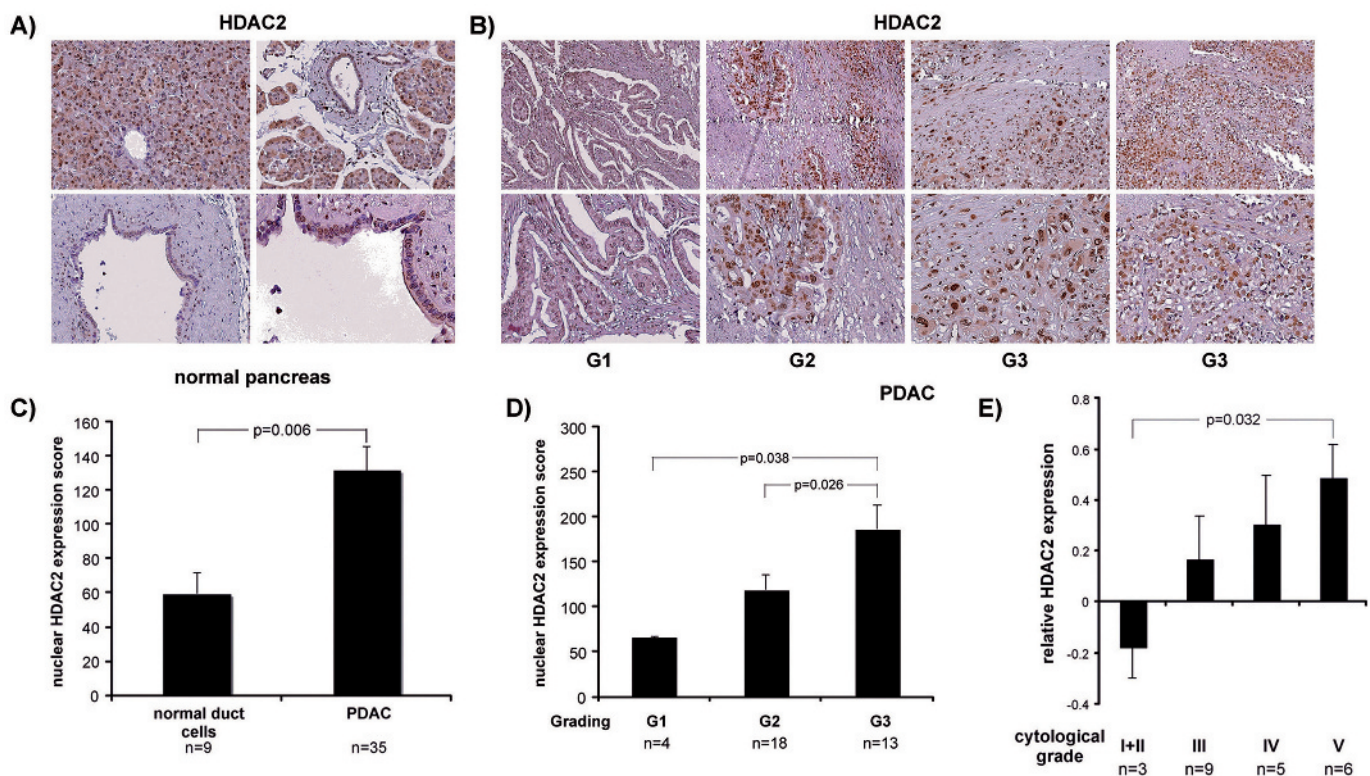


**Figure 1** HDAC2 is highly expressed in PDAC. (A) HDAC2 immunostaining of normal pancreatic parenchyma. (B) HDAC2 immunostaining of one well (G1), one moderately (G2) and two undifferentiated (G3) PDAC. Magnification: upper row,  $\times 100$ ; lower row,  $\times 200$ . (C) Nuclear HDAC2 score in normal duct cells and PDAC. The p value is indicated. (D) Nuclear HDAC2 score in well (G1), moderately (G2) and undifferentiated (G3) PDAC. The p value is indicated. (E) The Ishikawa microarray dataset (GEO accession number: GSE1542) was accessed using the OncoPrint™ Cancer Profiling Database and is plotted on a log scale. Data set contains HDAC2 expression according to the cytological grade. The p value is indicated. HDAC, histone deacetylase; PDAC, pancreatic ductal adenocarcinoma.

VPA was also observed in viability assays 72 h after the co-treatment with etoposide of MiaPaCa2 and Panc1 cells (fig 5B). In caspase 3/7 assays, etoposide induced a 4.6-fold increase of caspase 3/7 activity in MiaPaCa2 cells and a 3.1-fold increase of caspase 3/7 activity in Panc1 cells (fig 5C). This caspase activation was augmented by the co-treatment with VPA resulting in a 7.5-fold increase in MiaPaCa2 and a 5.1-fold increase in Panc1 cells (fig 5C). In contrast, neither VPA treatment nor RNAi-mediated depletion of HDAC2 considerably sensitised MiaPaCa2 and Panc1 cells towards gemcitabine (fig 5D,E), 5-FU (supplementary fig 2) or oxaliplatin (supplementary fig 3). These data confirmed the observations obtained with the HDAC2 siRNA, suggesting that HDAC2 inhibition results in specific sensitisation towards DNA damage-induced apoptosis.

### HDAC2 controls NOXA gene expression

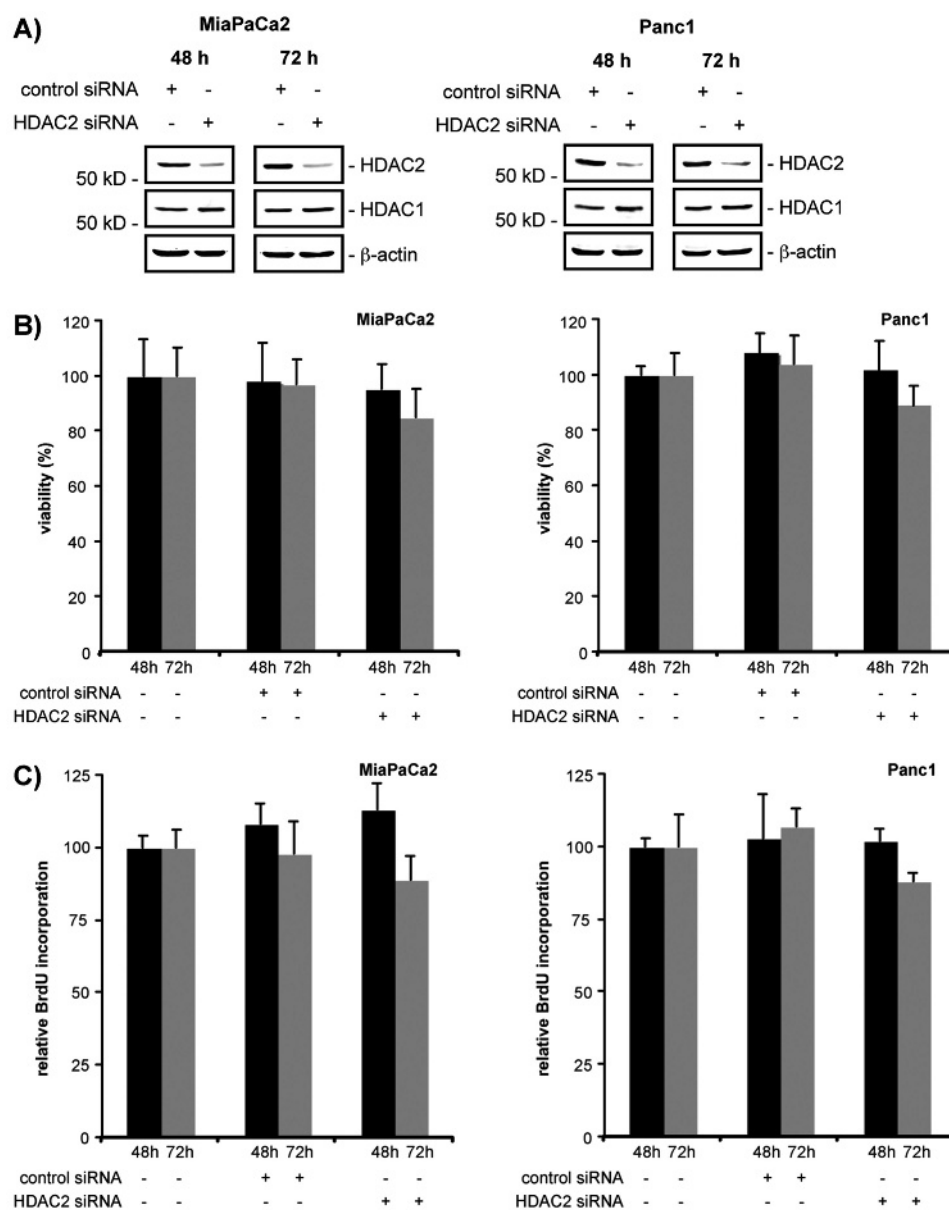
To find genes involved in the observed sensitisation towards intrinsic apoptosis we performed transcriptome profiling. Table 1 shows regulation of genes with known function in apoptosis. Among these genes, only the NOXA gene was significantly upregulated in MiaPaCa2 as well as in Panc1 cells after the HDAC2 knockdown. Since NOXA is involved in the apoptotic initiation upon etoposide treatment, we focused on its role in HDAC2-dependent sensitisation towards etoposide.<sup>24 25</sup> To validate the microarray data we used quantitative RT-PCR. As shown in fig 6A, NOXA mRNA was upregulated 4.4-fold in MiaPaCa2 cells and 2.2-fold in Panc1 cells 48 h after transfection of the HDAC2-specific siRNA compared to control siRNA-transfected cells. The knockdown of HDAC2 mRNA

was controlled by quantitative RT-PCR (fig 6A). Also, VPA treatment induced NOXA mRNA expression in both cell lines in a dose-dependent manner (fig 6B). As control, regulation of HDAC2 mRNA upon VPA treatment reached no statistical significance in both cell lines (fig 6B). Furthermore, NOXA mRNA expression was only marginally induced in PDAC cells after HDAC1 knockdown (supplementary fig 4). The VPA-induced increase of NOXA mRNA was paralleled by an equal increase of NOXA promoter activity (fig 6C). In ChIP assays direct and specific binding of HDAC2 to the NOXA locus in MiaPaCa2 and Panc1 cells was observed (fig 6D). Furthermore, we observed increased binding of acetylated histone H3 and RNA polymerase II to the NOXA promoter 48 h after HDAC2 depletion in MiaPaCa2 and Panc1 cells, arguing for an open chromatin structure and transcriptional upregulation. No change in binding of acetylated histone H3 or RNA polymerase II to the glyceraldehyde-3-phosphate dehydrogenase (GAPDH) promoter was observed, demonstrating specificity (fig 6D). Fitting to an open NOXA locus, we discovered pronounced and accelerated etoposide-induced NOXA mRNA expression in HDAC2-depleted MiaPaCa2 and Panc1 cells in a time-dependent manner (fig 6E).

### NOXA is essential for HDAC2-dependent resistance towards etoposide

To prove the essential role of NOXA for the sensitisation towards etoposide-induced apoptosis after the HDAC2 knockdown, we transfected HDAC2 and NOXA siRNAs alone or in combination into MiaPaCa2 and Panc1 cells. Knockdown of

**Figure 2** HDAC2 is dispensable for viability and proliferation of PDAC cells. (A) Western blot analysis of HDAC2 and HDAC1 48 and 72 h after the transfection of MiaPaCa2 (left panel) and Panc1 cells (right panel) with a control siRNA or a HDAC2-specific siRNA.  $\beta$ -Actin controls equal protein loading. (B) MTT assay of MiaPaCa2 (left graph) and Panc1 cells (right graph) 48 and 72 h after the transfection of a control siRNA or a HDAC2-specific siRNA compared to untransfected control cells. (C) BrdU assay of MiaPaCa2 (left graph) and Panc1 cells (right graph) 48 and 72 h after the transfection of a control siRNA or a HDAC2-specific siRNA compared to untransfected control cells. BrdU, bromodeoxyuridine; HDAC, histone deacetylase; MTT, 3-(4,5-dimethylthiazol-2-yl)-2,5-diphenyltetrazolium bromide; PDAC, pancreatic ductal adenocarcinoma.



HDAC2 and NOXA was verified by western blot (fig 7D). Again, the apoptotic fraction in MiaPaCa2 and Panc1 cells was increased after the knockdown of HDAC2 in etoposide treated cells (fig 7A). When HDAC2 and NOXA were simultaneously depleted, the etoposide-induced apoptotic fraction was equal to the fraction of etoposide-treated control siRNA-transfected cells (fig 7A). To further validate these results, we performed MTT and caspase 3/7 assays. Treatment with etoposide for 48 h induced a 44.2% reduction of viability in MiaPaCa2 cells and a 25.4% reduction of viability in Panc1 cells (fig 7B). This etoposide-induced reduction of viability was significantly increased in MiaPaCa2 (65.0%) and Panc1 (36.9%) cells after transfection of the HDAC2 siRNA (fig 7B). In contrast, simultaneous transfection of HDAC2 and NOXA siRNAs decreased the etoposide-induced reduction of viability to 29.0% in MiaPaCa2 cells and to 21.9% in Panc1 cells, respectively. In caspase 3/7 assays, treatment of control siRNA-transfected cells with etoposide induced a 5.2-fold increase of caspase 3/7 activity in MiaPaCa2 cells and a 3.1-fold increase of caspase 3/7 activity in Panc1 cells (fig 7C). This

etoposide-dependent induction of caspase 3/7 activity was further increased in HDAC2-depleted MiaPaCa2 (8.7-fold) and Panc1 cells (6.2-fold). Again, simultaneous transfection with HDAC2 and NOXA siRNAs impaired etoposide-induced upregulation of caspase 3/7 activity to 2.3-fold in MiaPaCa2 and 2.6-fold in Panc1 cells (fig 7C). Augmented PARP cleavage in HDAC2 siRNA-transfected MiaPaCa2 and Panc1 cells was reduced to levels of control siRNA-transfected cells in HDAC2/NOXA siRNAs double-transfected cells (fig 7D). Furthermore, NOXA protein abundance was distinctly increased in HDAC2-depleted and etoposide-treated MiaPaCa2 and Panc1 cells (fig 7D). Since NOXA preferentially binds to the anti-apoptotic BCL2 family member MCL1, we investigated MCL1 regulation by western blot. As shown in fig 7D, MCL1 is depleted in cases of effective apoptosis induction and this depletion is prevented by the NOXA knockdown.

## DISCUSSION

Although HDACs contribute to the carcinogenesis of solid tumours, definitive HDAC-controlled molecular pathways that

## Pancreatic cancer

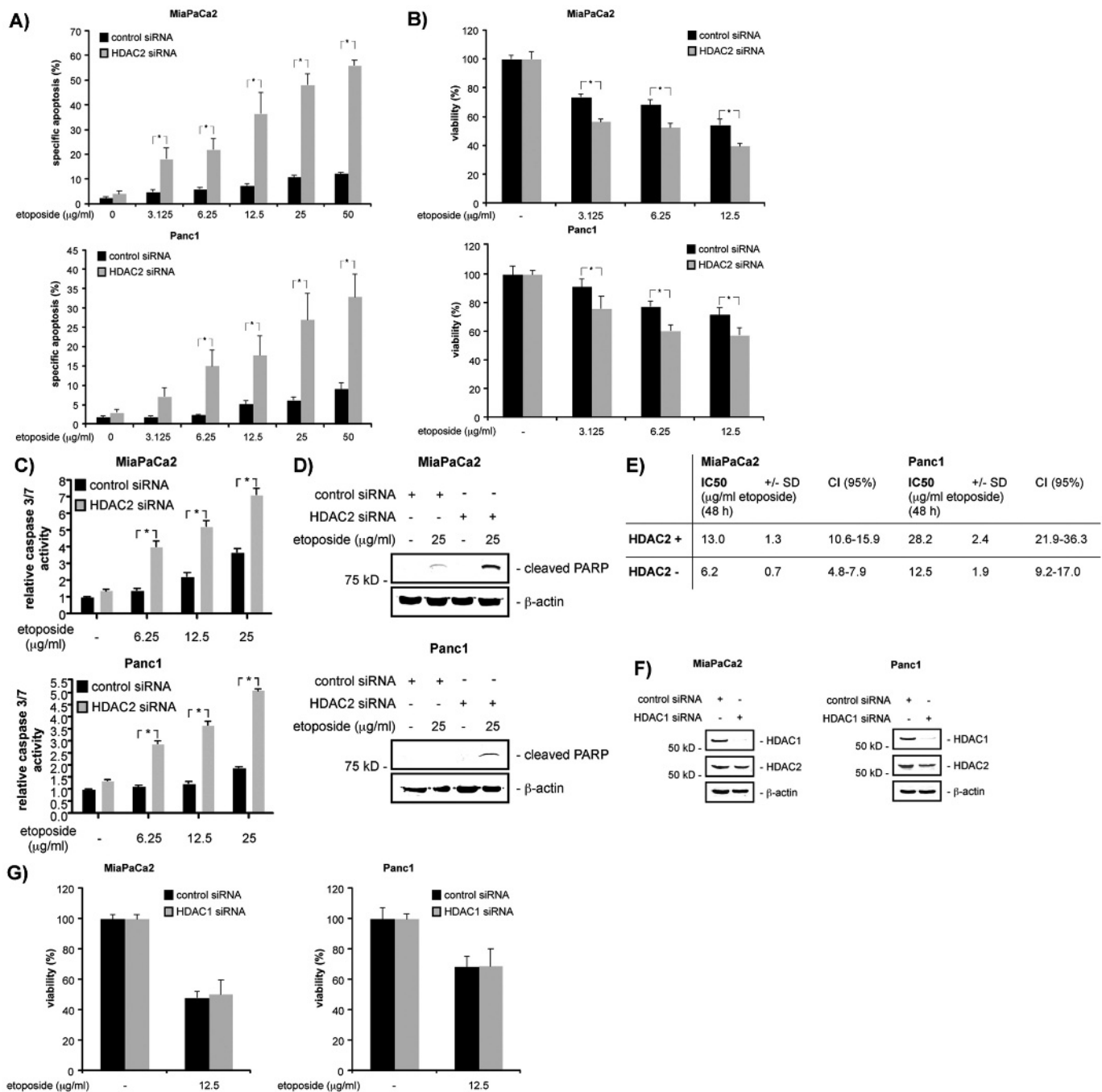
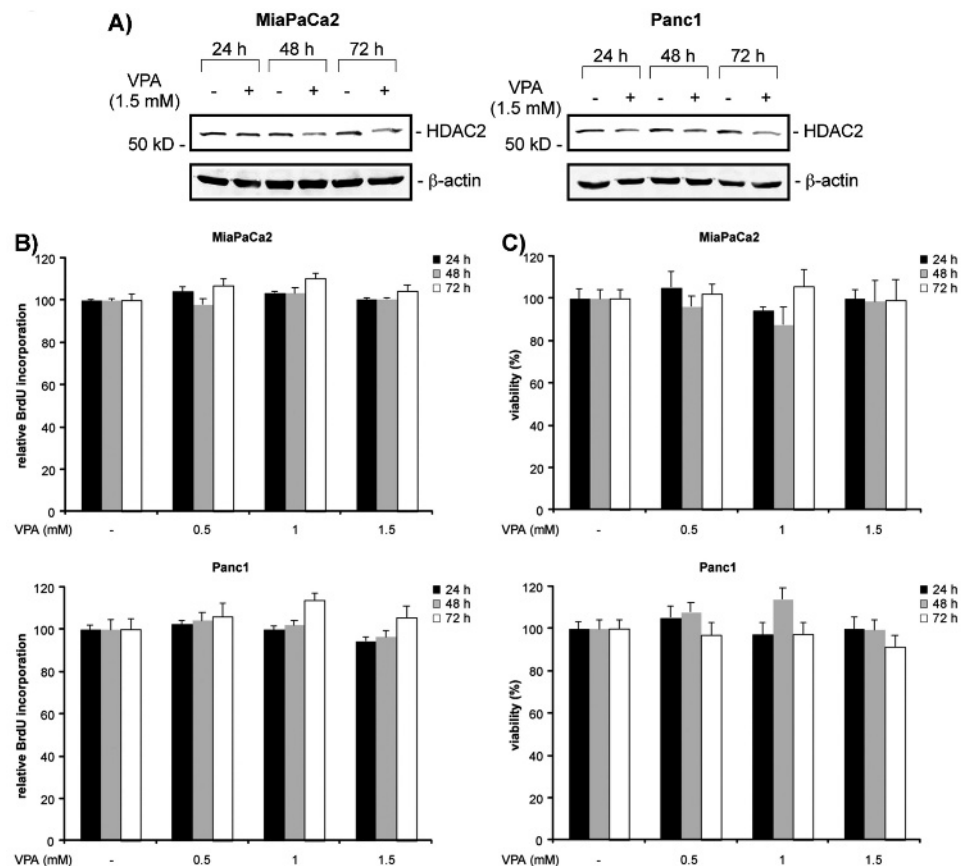


**Figure 3** Loss of HDAC2 sensitises PDAC cells towards etoposide-induced apoptosis. (A) MiaPaCa2 (upper graph) and Panc1 cells (lower graph) were transfected with a control siRNA or a HDAC2-specific siRNA. Forty-eight hours after transfection the cells were treated with increasing doses of etoposide, as indicated, for an additional 24 h or left as an untreated control. Apoptotic cells were quantified by fluorescence microscopy after Hoechst staining (Student t test: \* $p < 0.05$  vs controls). (B) MiaPaCa2 (upper graph) and Panc1 cells (lower graph) were transfected with a control siRNA or a HDAC2-specific siRNA. Twenty-four hours after the transfection the cells were treated with increasing doses of etoposide, as indicated, for an additional 48 h or left as an untreated control. Viability was determined using MTT assays (Student t test: \* $p < 0.05$  vs controls). (C) MiaPaCa2 (upper graph) and Panc1 cells (lower graph) were transfected with a control siRNA or a HDAC2-specific siRNA as indicated. Forty-eight hours after the transfection the cells were treated with different doses of etoposide, as indicated, for an additional 24 h or left as an untreated control. Caspase activity was measured using caspase 3/7 activity assays (Student t test: \* $p < 0.05$  vs controls). (D) MiaPaCa2 and Panc1 cells were transfected with a control siRNA or a HDAC2-specific siRNA. Forty-eight hours after the transfection the cells were treated with 25  $\mu\text{g/ml}$  etoposide for an additional 24 h or left as an untreated control. Cleaved PARP western blot was used as an indirect measurement of caspase activity.  $\beta$ -Actin controls equal protein loading. (E)  $\text{IC}_{50}$  values in MTT assays of control siRNA (HDAC2+) and HDAC2 siRNA-transfected (HDAC2-) MiaPaCa2 and Panc1 cells treated for 48 h with etoposide. (F) Western blot analysis of HDAC1 and HDAC2 expression 48 h after the transfection of MiaPaCa2 (left panel) and Panc1 cells (right panel) with a control siRNA or a HDAC1-specific siRNA.  $\beta$ -Actin controls equal protein loading. (G) MiaPaCa2 (left panel) and Panc1 cells (right panel) were transfected with a control siRNA or a HDAC1-specific siRNA. Twenty-four hours after the transfection the cells were treated with 12.5  $\mu\text{g/ml}$  etoposide, as indicated, for an additional 48 h or left as an untreated control. Viability was determined using MTT assays. HDAC, histone deacetylase; MTT, 3-(4,5-dimethylthiazol-2-yl)-2,5-diphenyltetrazolium bromide; PARP, poly (ADP-ribose) polymerase family, member 1; PDAC, pancreatic ductal adenocarcinoma.

**Figure 4** VPA treatment of PDAC cells does not impair proliferation or viability. (A) Western blot analysis of HDAC2 24, 48 and 72 h after the treatment of MiaPaCa2 (left panel) and Panc1 cells (right panel) with 1.5 mmol/l VPA. Controls were treated with vehicle alone.  $\beta$ -Actin controls equal protein loading.

(B) BrdU assay of MiaPaCa2 (upper graph) and Panc1 cells (lower graph) 24, 48 and 72 h after the treatment with VPA as indicated. Controls were treated with vehicle alone. (C) MTT assay of MiaPaCa2 (upper graph) and Panc1 cells (lower graph) 24, 48 and 72 h after the treatment with VPA as indicated. Controls were treated with vehicle alone. BrdU, bromodeoxyuridine; HDAC, histone deacetylase; MTT, 3-(4,5-dimethylthiazol-2-yl)-2,5-diphenyltetrazolium bromide; PDAC, pancreatic ductal adenocarcinoma; VPA, valproic acid.



allow assessment of relevant biological responses and isoenzyme specific functions as a basis for the improvement of isoenzyme selectivity of future HDACi are ill defined. In this study, we characterised a novel HDAC2-dependent pathway, where HDAC2-mediated silencing of the NOXA gene contributes to resistance against topoisomerase II inhibitor treatment in PDAC cells.

As in other gastrointestinal tumours, such as colon and gastric cancer, we demonstrate over-expression of HDAC2 in human PDAC.<sup>26-29</sup> Furthermore, we observed increased nuclear HDAC2 expression already in pancreatic intraepithelial neoplasias (PanINs) in a murine *Kras*<sup>G12D</sup>-dependent PDAC model (data not shown). Therefore, over-expression of HDAC2 suggests a key role of HDAC2 in gastrointestinal carcinogenesis. Consistently, an essential contribution of HDAC2 towards the carcinogenesis of gastrointestinal tumours was recently proved in an APC<sup>min</sup> mouse model of colon cancer in vivo.<sup>30</sup>

The functions of HDAC2 are highly cell type and tissue specific. In vivo, a recent report demonstrates that HDAC2 knockout mice are characterised by increased cardiac cell proliferation and apoptosis, a phenotype that was not observed in non-cardiac tissues.<sup>31</sup> In contrast to in vitro studies in various cancer cell lines, we did not find reduced proliferation, cell viability or increased apoptosis upon RNAi-mediated HDAC2 depletion, arguing for a redundant function of HDAC2 towards cell cycle progression and apoptosis induction in PDAC cells.<sup>26 27 29 32 33</sup> The observation that treatment of PDAC cells with the more class I-restricted HDACi VPA has no effect on proliferation and viability points to a contribution of class II or IV HDACs.

As a non-redundant function of HDAC2 we observed a marked sensitisation towards the topoisomerase II inhibitor etoposide, since sensitisation towards etoposide was not

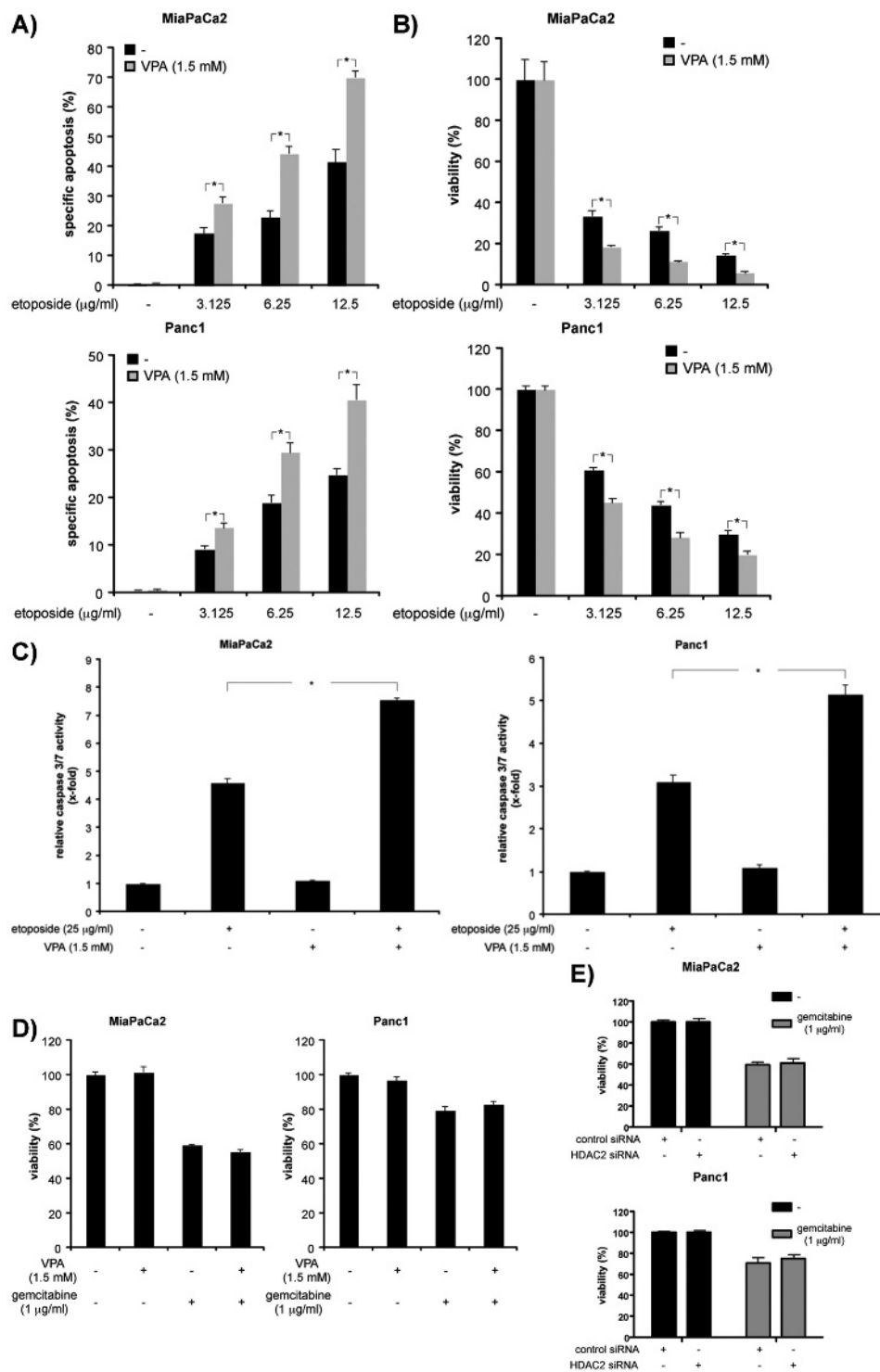
observed in HDAC1 siRNA-transfected PDAC cells. This notion is also suggested by the almost identical induction of NOXA mRNA expression in HDAC2 siRNA-transfected and VPA-treated PDAC cells. In addition to the sensitising effect towards etoposide, recent evidence suggests a synergy of HDAC2 depletion with antihormone therapy in breast cancer cells and with death-receptor activation in colon cancer cells, demonstrating the importance of HDAC2 as a therapeutic target.<sup>34 35</sup>

The synergy of the class I HDACi/topoisomerase II inhibitor combination in vitro and in vivo is well documented and anti-tumour activity was observed in a recent phase I trial in advanced solid tumours using VPA and epirubicin. Nevertheless, the molecular mechanisms explaining the synergy and the contributing HDAC isoenzymes are ill defined.<sup>36-39</sup> Our results now demonstrate that the NOXA gene is an important downstream target explaining the mode of action of the HDACi/topoisomerase II inhibitor combination at the molecular level in PDAC cells. In transcriptome profiling experiments we found an upregulation of the mRNA of the BH3-only protein NOXA in HDAC2-depleted PDAC cells. Furthermore, increased NOXA mRNA expression was also observed after VPA treatment. BH3-only proteins, receptors of cellular stress and most apical regulators of apoptosis, induce, once activated, mitochondrial membrane permeabilisation and the release of pro-apoptotic factors.<sup>40</sup> Since HDAC2 depletion-mediated sensitisation towards etoposide is completely impeded by the RNAi-induced knock-down of NOXA, HDAC2-mediated regulation of the NOXA gene is sufficient to explain the observed synergism. In this pathway, the NOXA gene locus is controlled by HDAC2, since HDAC2 depletion results in specific acetylation of histone H3 at the NOXA locus, demonstrating opening of the chromatin.

## Pancreatic cancer

**Figure 5** VPA and etoposide synergise to induce apoptosis of PDAC cells.

(A) MiaPaCa2 (upper graph) and Panc1 cells (lower graph) were co-treated with VPA and etoposide for 48 h as indicated. Apoptotic cells were quantified by fluorescence microscopy after Hoechst staining (Student t test:  $*p < 0.05$  vs controls). (B) MiaPaCa2 (upper graph) and Panc1 cells (lower graph) were co-treated with VPA and etoposide for 72 h as indicated. Viability was measured by MTT assays (Student t test:  $*p < 0.05$  vs controls). (C) MiaPaCa2 (left graph) and Panc1 cells (right graph) were treated with VPA (1.5 mmol/l), etoposide (25  $\mu$ g/ml) or co-treated with VPA and etoposide for 24 h as indicated. Caspase activity was measured using caspase 3/7 activity assays (Student t test:  $*p < 0.05$  vs controls). (D) MiaPaCa2 (left graph) and Panc1 cells (right graph) were co-treated with VPA and gemcitabine for 48 h as indicated. Viability was measured using MTT assays. (E) MiaPaCa2 (upper graph) and Panc1 cells (lower graph) were transfected with a control siRNA or a HDAC2-specific siRNA. Twenty-four hours after the transfection the cells were treated with gemcitabine as indicated for an additional 48 h or left as an untreated control. Viability was determined using MTT assays. MTT, 3-(4,5-dimethylthiazol-2-yl)-2,5-diphenyltetrazolium bromide; PDAC, pancreatic ductal adenocarcinoma; VPA, valproic acid.



NOXA was identified as a phorbol ester-inducible and p53-regulated gene that is involved in apoptosis upon genotoxic stress.<sup>41-42</sup> This was validated in mouse embryonic fibroblasts of NOXA-deficient mice, which demonstrate a higher threshold for etoposide-induced apoptosis.<sup>24-25</sup> Furthermore, adenoviral transfer of wild-type p53 combined with HDACi treatment synergises to induce NOXA protein expression and apoptosis in the gastric cancer cell line MKN45, suggesting that NOXA expression is epigenetically silenced in an HDAC-dependent manner, and validating the importance of p53 in NOXA gene activation.<sup>43</sup> Since HDAC2 can repress DNA binding of p53 to

relevant target genes in MCF7 cells, a p53-dependent activation of NOXA after the HDAC2 knockdown has to be considered in our model system.<sup>33</sup> Nevertheless, this scenario is unlikely, since MiaPaCa2 as well as Panc1 cells express p53 proteins with mutations in the DNA-binding domain. The relevant transcription factors in our model system are unknown so far and ongoing experiments beyond the scope of the current manuscript try to address this topic.

Recent investigations demonstrate an upregulation of NOXA protein and mRNA abundance after treatment of leukaemic cells with HDACi and the contribution of NOXA for HDACi-induced



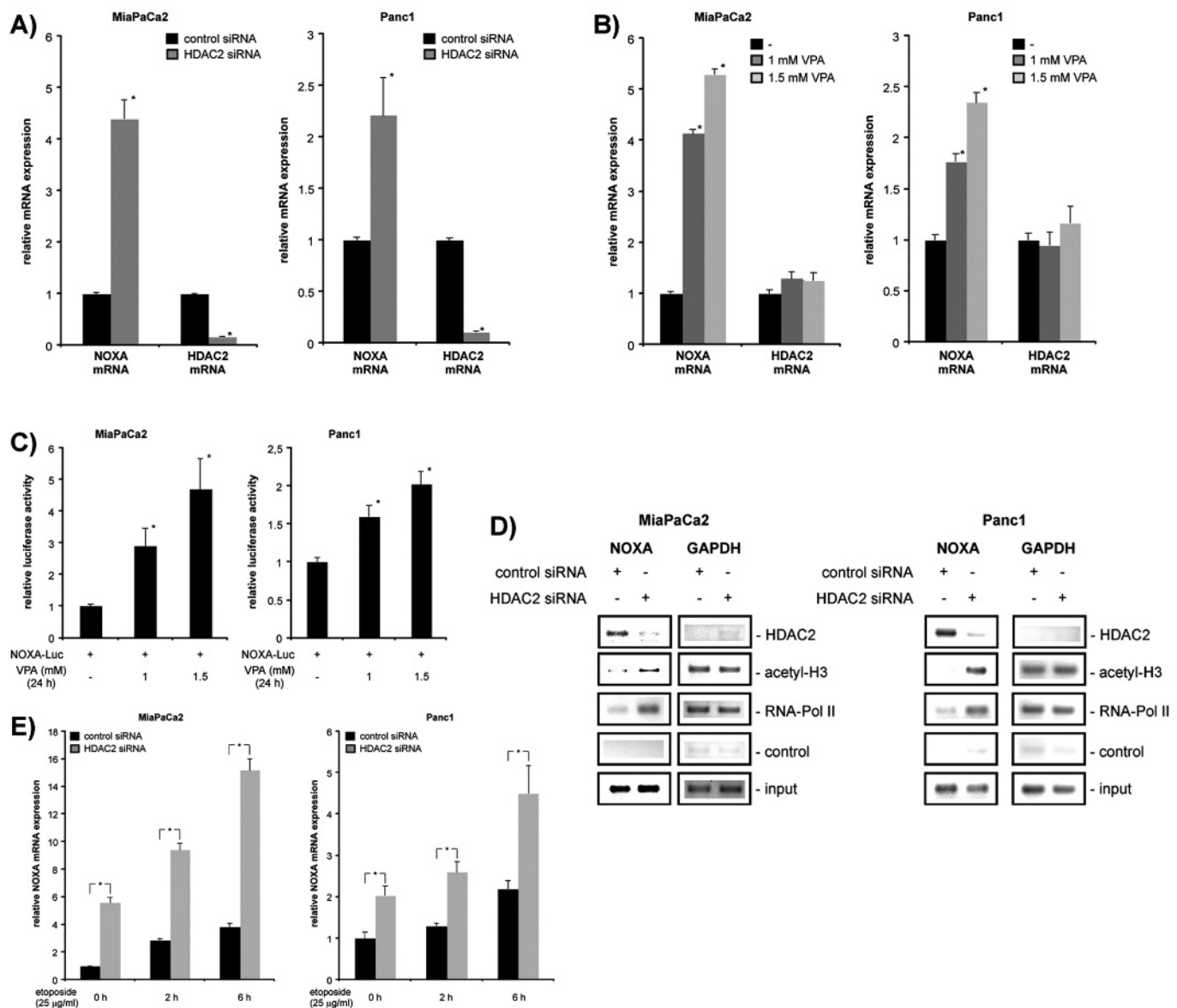


**Figure 6** HDAC2 represses the NOXA gene. (A) Quantitative NOXA and HDAC2 mRNA expression analysis in MiaPaCa2 (left graph) and Panc1 cells (right graph) after HDAC2 siRNA transfection. Total RNA was prepared 48 h post-transfection. NOXA and HDAC2 mRNA levels were quantified using real-time PCR analysis and normalised to cyclophilin expression levels. (B) Quantitative NOXA and HDAC2 mRNA expression analysis in MiaPaCa2 (left graph) and Panc1 cells (right graph) after VPA treatment. Total RNA was prepared 48 h after the treatment with VPA as indicated. NOXA and HDAC2 mRNA levels were quantified using real-time PCR analysis and normalised to cyclophilin expression levels. (C) NOXA-Luc reporter gene (500 ng) was transfected into MiaPaCa2 (left graph) and Panc1 cells (right graph). Twenty-four hours after the transfection the cells were treated with VPA as indicated or were left as an untreated control. Twenty-four hours after the VPA treatment, luciferase activity was measured (Student t test: \* $p < 0.05$  vs control). (D) Chromatin immunoprecipitation analysis of the NOXA gene. Chromatin of MiaPaCa2 (left graph) and Panc1 cells (right graph) transfected with a control siRNA or a HDAC2-specific siRNA was immunoprecipitated with a HDAC2-, a RNA polymerase II- or an acetylated-histone H3-specific antibody or IgG as negative control. Precipitated DNA or 10% of the chromatin input was amplified with gene specific primers for NOXA or GAPDH as a control. (E) Quantitative NOXA mRNA expression analysis in MiaPaCa2 (left graph) and Panc1 cells (right graph). Forty-eight hours after the HDAC2 or control siRNA transfection, cells were treated with 25  $\mu\text{g/ml}$  etoposide or were left as an untreated control. Total RNA was prepared at the indicated time points and NOXA mRNA levels were quantified using real-time PCR analysis and normalised to cyclophilin expression levels. HDAC, histone deacetylase; PCR, polymerase chain reaction; VPA, valproic acid.

apoptosis.<sup>44, 45</sup> In contrast to these studies, we observed no overt induction of apoptosis in HDAC2-depleted or VPA-treated PDAC cells, which might be explained by differences in carcinogenesis and tumour biology of leukaemia and PDAC. Furthermore, the lack of correlation between increased NOXA mRNA and protein observed in MiaPaCa2 cells and the lack of depletion of the MCL1 protein in Panc1 cells after HDAC2 depletion might explain the observation that only HDAC2 targeting fails to induce apoptosis.

Although VPA is less potent than newer generation HDACi, the well-known toxicity profile, long-term safety data, cost-effectiveness and good tissue penetrance argue for testing VPA in further clinical trials, especially in combination with cytotoxic drugs.<sup>46</sup> Since our data demonstrate that NOXA is a relevant HDACi target, NOXA activating agents, like topoisomerase II inhibitors or proteasome inhibitors, should be considered for the design of novel VPA/HDACi combinations. This is especially important

## Pancreatic cancer

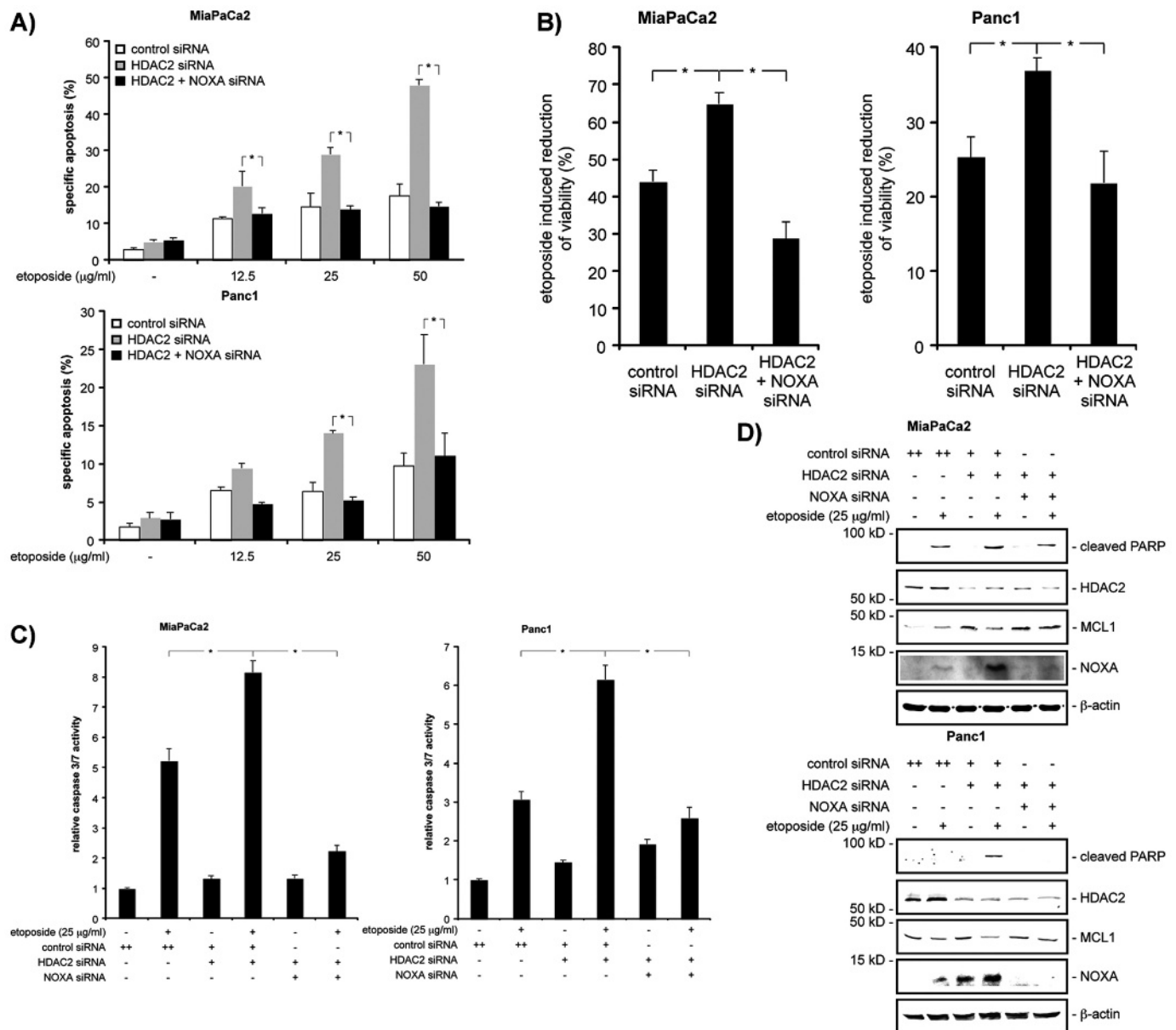


**Figure 7** NOXA is essential for HDAC2 knockdown-dependent sensitisation towards etoposide. (A) MiaPaCa2 (upper graph) and Panc1 cells (lower graph) were transfected with a control siRNA, a HDAC2-specific siRNA or co-transfected with a HDAC2- and NOXA-specific siRNAs as indicated. Forty-eight hours after the transfection the cells were treated with increasing doses of etoposide, as indicated, for an additional 24 h or left as an untreated control. Apoptotic cells were quantified by fluorescence microscopy after Hoechst staining (Student t test: \* $p < 0.05$  vs controls). (B) MiaPaCa2 (left graph) and Panc1 cells (right graph) were transfected with a control siRNA, a HDAC2-specific siRNA or co-transfected with HDAC2- and NOXA-specific siRNAs as indicated. Twenty-four hours after the transfection the cells were treated with 12.5  $\mu\text{g/ml}$  etoposide for an additional 48 h or left as an untreated control. Etoposide-induced reduction of viability was measured using MTT assays (Student t test: \* $p < 0.05$  vs controls). (C) MiaPaCa2 (left graph) and Panc1 cells (right graph) were transfected with a control siRNA, a HDAC2-specific siRNA or co-transfected with HDAC2- and NOXA-specific siRNAs as indicated. Forty-eight hours after the transfection the cells were treated with 25  $\mu\text{g/ml}$  etoposide for an additional 24 h or left as an untreated control. Caspase activity was measured using caspase 3/7 activity assays (Student t test: \* $p < 0.05$  vs controls). (D) MiaPaCa2 (upper panel) and Panc1 cells (lower panel) were transfected with a control siRNA, a HDAC2-specific siRNA or co-transfected with HDAC2- and NOXA-specific siRNAs as indicated. Forty-eight hours after the transfection the cells were treated with 25  $\mu\text{g/ml}$  etoposide for an additional 24 h or left as an untreated control. Western blot analysis demonstrates expression of cleaved PARP, HDAC2, MCL1 and NOXA.  $\beta$ -Actin controls equal protein loading. HDAC, histone deacetylase; MTT, 3-(4,5-dimethylthiazol-2-yl)-2,5-diphenyltetrazolium bromide.

since we were not able to demonstrate synergy between HDAC2 depletion or VPA treatment with current standard chemotherapeutics, such as gemcitabine or 5-FU.

Together, we have characterised a novel HDAC2- and NOXA-dependent pathway of therapeutic resistance in PDAC, which may be the basis for the development of novel therapeutic strategies.

**Acknowledgements:** We thank Drs Häcker and Krämer for discussions, Dr Lallemand for providing the NOXA promoter, Dr Mages for microarray support, and Mesdames Hoffmann, Netz and Kohne-Ertel for excellent technical support.

**Funding:** DFG (Grant SCHN 959/1-1) and Else Kröner-Fresenius Stiftung (Grant A130/07).

**Competing interests:** None.

**Provenance and peer review:** Not commissioned; externally peer reviewed.

## REFERENCES

- Schneider G, Siveke JT, Eckel F, *et al*. Pancreatic cancer: basic and clinical aspects. *Gastroenterology* 2005;**128**:1606–25.
- Fulda S, Debatin KM. Extrinsic versus intrinsic apoptosis pathways in anticancer chemotherapy. *Oncogene* 2006;**25**:4798–811.
- Hamacher R, Schmid RM, Saur D, *et al*. Apoptotic pathways in pancreatic ductal adenocarcinoma. *Mol Cancer* 2008;**7**:64.
- Yang XJ, Seto E. The Rpd3/Hda1 family of lysine deacetylases: from bacteria and yeast to mice and men. *Nat Rev Mol Cell Biol* 2008;**9**:206–18.
- Minucci S, Pellicci PG. Histone deacetylase inhibitors and the promise of epigenetic (and more) treatments for cancer. *Nat Rev Cancer* 2006;**6**:38–51.
- Glozak MA, Seto E. Histone deacetylases and cancer. *Oncogene* 2007;**26**:5420–32.
- Bolden JE, Peart MJ, Johnstone RW. Anticancer activities of histone deacetylase inhibitors. *Nat Rev Drug Discov* 2006;**5**:769–84.
- Donadelli M, Costanzo C, Faggioli L, *et al*. Trichostatin A, an inhibitor of histone deacetylases, strongly suppresses growth of pancreatic adenocarcinoma cells. *Mol Carcinogenesis* 2003;**38**:59–69.
- Sato N, Ohta T, Kitagawa H, *et al*. FR901228, a novel histone deacetylase inhibitor, induces G2-M cell cycle arrest and subsequent apoptosis in refractory human pancreatic cancer cells. *Int J Oncol* 2004;**24**:679–85.
- Ryu JK, Lee WJ, Lee KH, *et al*. SK-7041, a new histone deacetylase inhibitor, induces G2-M cell cycle arrest and apoptosis in pancreatic cancer cell lines. *Cancer Lett* 2006;**237**:143–54.
- Ammerpohl O, Trauzold A, Schniewind B, *et al*. Complementary effects of HDAC inhibitor 4-PB on gap junction communication and cellular export mechanisms support restoration of chemosensitivity of PDAC cells. *Br J Cancer* 2007;**96**:73–81.
- Kumagai T, Wakimoto N, Yin D, *et al*. Histone deacetylase inhibitor, suberoylanilide hydroxamic acid (Vorinostat, SAHA) profoundly inhibits the growth of human pancreatic cancer cells. *Int J Cancer* 2007;**121**:656–65.
- Neureiter D, Zopf S, Leu T, *et al*. Apoptosis, proliferation and differentiation patterns are influenced by Zebularine and SAHA in pancreatic cancer models. *Scand J Gastroenterol* 2007;**42**:103–16.
- Ouaissi M, Cabral S, Tavares J, *et al*. Histone deacetylase (HDAC) encoding gene expression in pancreatic cancer cell lines and cell sensitivity to HDAC inhibitors. *Cancer Biol Ther* 2008;**7**:523–31.
- Schneider G, Reichert M, Saur D, *et al*. HDAC3 is linked to cell cycle machinery in MiaPaCa2 cells by regulating transcription of *skp2*. *Cell Prolif* 2007;**40**:522–31.
- Piacentini P, Donadelli M, Costanzo C, *et al*. Trichostatin A enhances the response of chemotherapeutic agents in inhibiting pancreatic cancer cell proliferation. *Virchows Arch* 2006;**448**:797–804.
- Donadelli M, Costanzo C, Beghelli S, *et al*. Synergistic inhibition of pancreatic adenocarcinoma cell growth by trichostatin A and gemcitabine. *Biochim Biophys Acta* 2007;**1773**:1095–106.
- Reichert M, Saur D, Hamacher R, *et al*. Phosphoinositide-3-kinase signaling controls S-phase kinase-associated protein 2 transcription via E2F1 in pancreatic ductal adenocarcinoma cells. *Cancer Res* 2007;**67**:4149–56.
- Lallemand C, Blanchard B, Palmieri M, *et al*. Single-stranded RNA viruses inactivate the transcriptional activity of p53 but induce NOXA-dependent apoptosis via post-translational modifications of IRF-1, IRF-3 and CREB. *Oncogene* 2007;**26**:328–38.
- Seidler B, Schmidt A, Mayr U, *et al*. A Cre-loxP-based mouse model for conditional somatic gene expression and knockdown in vivo by using avian retroviral vectors. *Proc Natl Acad Sci U S A* 2008;**105**:10137–42.
- Ishikawa M, Yoshida K, Yamashita Y, *et al*. Experimental trial for diagnosis of pancreatic ductal carcinoma based on gene expression profiles of pancreatic ductal cells. *Cancer Sci* 2005;**96**:387–93.
- Gottlicher M, Minucci S, Zhu P, *et al*. Valproic acid defines a novel class of HDAC inhibitors inducing differentiation of transformed cells. *Embo J* 2001;**20**:6969–78.
- Kramer OH, Zhu P, Ostendorff HP, *et al*. The histone deacetylase inhibitor valproic acid selectively induces proteasomal degradation of HDAC2. *Embo J* 2003;**22**:3411–20.
- Shibue T, Takeda K, Oda E, *et al*. Integral role of Noxa in p53-mediated apoptotic response. *Genes Dev* 2003;**17**:2233–8.
- Villunger A, Michalak EM, Coultas L, *et al*. p53- and drug-induced apoptotic responses mediated by BH3-only proteins puma and noxa. *Science* 2003;**302**:1036–8.
- Zhu P, Martin E, Mengwasser J, *et al*. Induction of HDAC2 expression upon loss of APC in colorectal tumorigenesis. *Cancer Cell* 2004;**5**:455–63.
- Huang BH, Laban M, Leung CH, *et al*. Inhibition of histone deacetylase 2 increases apoptosis and p21Cip1/WAF1 expression, independent of histone deacetylase 1. *Cell Death Differ* 2005;**12**:395–404.
- Weichert W, Roske A, Gekeler V, *et al*. Association of patterns of class I histone deacetylase expression with patient prognosis in gastric cancer: a retrospective analysis. *Lancet Oncol* 2008;**9**:139–48.
- Weichert W, Roske A, Niesporek S, *et al*. Class I histone deacetylase expression has independent prognostic impact in human colorectal cancer: specific role of class I histone deacetylases in vitro and in vivo. *Clin Cancer Res* 2008;**14**:1669–77.
- Zimmermann S, Kiefer F, Prudenziati M, *et al*. Reduced body size and decreased intestinal tumor rates in HDAC2-mutant mice. *Cancer Res* 2007;**67**:9047–54.
- Montgomery RL, Davis CA, Potthoff MJ, *et al*. Histone deacetylases 1 and 2 redundantly regulate cardiac morphogenesis, growth, and contractility. *Genes Dev* 2007;**21**:1790–802.
- Wilson AJ, Byun DS, Popova N, *et al*. Histone deacetylase 3 (HDAC3) and other class I HDACs regulate colon cell maturation and p21 expression and are deregulated in human colon cancer. *J Biol Chem* 2006;**281**:13548–58.
- Harms KL, Chen X. Histone deacetylase 2 modulates p53 transcriptional activities through regulation of p53-DNA binding activity. *Cancer Res* 2007;**67**:3145–52.
- Bicaku E, Marchion DC, Schmitt ML, *et al*. Selective inhibition of histone deacetylase 2 silences progesterone receptor-mediated signaling. *Cancer Res* 2008;**68**:1513–9.
- Kaler P, Sasazuki T, Shirasawa S, *et al*. HDAC2 deficiency sensitizes colon cancer cells to TNFalpha-induced apoptosis through inhibition of NF-kappaB activity. *Exp Cell Res* 2008;**314**:1507–18.
- Tsai SC, Valkov N, Yang WM, *et al*. Histone deacetylase interacts directly with DNA topoisomerase II. *Nat Genet* 2000;**26**:349–53.
- Marchion DC, Bicaku E, Daud AI, *et al*. In vivo synergy between topoisomerase II and histone deacetylase inhibitors: predictive correlates. *Mol Cancer Ther* 2005;**4**:1993–2000.
- Marchion DC, Bicaku E, Turner JG, *et al*. Synergistic interaction between histone deacetylase and topoisomerase II inhibitors is mediated through topoisomerase IIbeta. *Clin Cancer Res* 2005;**11**:8467–75.
- Munster P, Marchion D, Bicaku E, *et al*. Phase I trial of histone deacetylase inhibition by valproic acid followed by the topoisomerase II inhibitor epirubicin in advanced solid tumors: a clinical and translational study. *J Clin Oncol* 2007;**25**:1979–85.
- Hacker G, Weber A. BH3-only proteins trigger cytochrome c release, but how? *Arch Biochem Biophys* 2007;**462**:150–5.
- Hijikata M, Kato N, Sato T, *et al*. Molecular cloning and characterization of a cDNA for a novel phorbol-12-myristate-13-acetate-responsive gene that is highly expressed in an adult T-cell leukemia cell line. *J Virol* 1990;**64**:4632–9.
- Oda E, Ohki R, Murasawa H, *et al*. Noxa, a BH3-only member of the Bcl-2 family and candidate mediator of p53-induced apoptosis. *Science* 2000;**288**:1053–8.
- Sasaki Y, Negishi H, Idogawa M, *et al*. Histone deacetylase inhibitor FK228 enhances adenovirus-mediated p53 family gene therapy in cancer models. *Mol Cancer Ther* 2008;**7**:779–87.
- Inoue S, Riley J, Gant TW, *et al*. Apoptosis induced by histone deacetylase inhibitors in leukemic cells is mediated by Bim and Noxa. *Leukemia* 2007;**21**:1773–82.
- Inoue S, Walewska R, Dyer MJ, *et al*. Downregulation of Mcl-1 potentiates HDACi-mediated apoptosis in leukemic cells. *Leukemia* 2008;**22**:819–25.
- Duenas-Gonzalez A, Candelaria M, Perez-Plascencia C, *et al*. Valproic acid as epigenetic cancer drug: preclinical, clinical and transcriptional effects on solid tumors. *Cancer Treat Rev* 2008;**34**:206–22.



## HDAC2 mediates therapeutic resistance of pancreatic cancer cells via the BH3-only protein NOXA

P Fritsche, B Seidler, S Schüler, A Schnieke, M Göttlicher, R M Schmid, D Saur and G Schneider

*Gut* 2009 58: 1399-1409 originally published online June 14, 2009  
doi: 10.1136/gut.2009.180711

---

Updated information and services can be found at:  
<http://gut.bmj.com/content/58/10/1399>

*These include:*

### Supplementary Material

Supplementary material can be found at:  
<http://gut.bmj.com/content/suppl/2009/10/02/gut.2009.180711.DC1.html>

### References

This article cites 46 articles, 18 of which you can access for free at:  
<http://gut.bmj.com/content/58/10/1399#BIBL>

### Email alerting service

Receive free email alerts when new articles cite this article. Sign up in the box at the top right corner of the online article.

---

### Topic Collections

Articles on similar topics can be found in the following collections

[Pancreas and biliary tract](#) (1942)  
[Pancreatic cancer](#) (655)

---

### Notes

---

To request permissions go to:  
<http://group.bmj.com/group/rights-licensing/permissions>

To order reprints go to:  
<http://journals.bmj.com/cgi/reprintform>

To subscribe to BMJ go to:  
<http://group.bmj.com/subscribe/>